Journal of Harbin Engineering University
ISSN: 1006-7043

Vol 44 No. 8
August 2023

Occluded Face Recognition: Contrast Correction & Edge Preserving Enhancement based Optimum Features on CelebA Dataset

[1]Mahadeo D Narlawar,

Datta Meghe College of Engineering, Airoli, Navi Mumbai, University of Mumbai India,
narlawaratul@gmail.com

[2]DR. D. J. Pete,

Datta Meghe College of Engineering, Airoli, Navi Mumbai, University of Mumbai India,
dnyandeo.pete@dmce.ac.in

Abstract

The challenging task of human face identification under variety of occlusions has been interesting and concentrated topic today. The ability of most of the recognition systems drops drastically due to large occluded region and less unoccluded areas. We present an efficient pre-processing and optimum features based occluded face classification system. The occlusions included in the dataset are pose, illumination, age, expressions, hair over face and extend to 40 such difficulties. The pre-processing stage involves two parallel processes and includes contrast measurement-correction and edge-preserving enhancement for the occluded face images. Optimum fine textural features are extracted using Gabor coefficients, Linear Binary Patterns based on Haar Wavelet components and Histogram of Gaussian features. Statistical global features based on first order, wavelet components and color histograms forms the other set of features to represent the whole occluded face region. The work considers 100 celebrities from the CelebA dataset with pose and other occlusions to validate using support vector machine. Experiments analysis carried using the proposed efficient pre-processing and optimum features based face identification system showed improved classification accuracy over other well-known techniques.

Keywords - face identification, occlusion, efficient pre-processing and optimum features, contrast measurement-correction, edge-preserving enhancement, textural features and statistical features.

Introduction

Increasing large public face data sets had attributed to focused development in human computer interface for access control system. Many existing face recognition systems found in the literature are aimed developing systems under general conditions and gained wide popularity due to their performance. Some of the recognition systems even have the ability to override human recognition over some of the publicly available face datasets [1]. However when the faces are subjected to diverse conditions like pose, illumination conditions or being occluded, the ability of most of the recognition systems drops drastically [2-3]. Occluded faces due to intentional or unintentional obstacles over the face such as moustache, beard, mask, hands, and spectacles degrade the performance of common face detection models. Still, work presented in [4-5] aimed to improve face detection models under occluded faces. As seen from the latest datasets made available over the globe shows various challenging aspects over the faces than the traditional face datasets. Due to insufficient occluded face datasets and the generalization ability of existing face recognition models imposes bottleneck in solving the problem. Although many such works have been suggested to handle the occluded challenge, issues like expressions, age, pose are still are large.

The ability of detection models for real world occluded faces basically is governed by robust feature extraction process and the classifier. Many remarkable methods have been developed in the past decades incorporating principal component analysis [6], local binary patterns and their variants [7], linear discriminant

analysis [8] etc. using classifiers such as support vector machine [9], kernel linear discriminant analysis [10] and others. These methods are remarkable when projected over traditional face datasets but their performance degrades over occluded faces. Rajeshwari and Ithaya Rani [11] proposed two stage machine learning approach for removal of occlusion using structural similarity index measure and PCA. In the first stage they acquired the necessary information from the lost face region using the face similar matrix to generate related face followed by generating the Eigen spaces using PCA to regenerate the occluded area in the later stage. Yueying Li [12] suggested a double channel perceptron neural network where VGG16 was used as a judgement unit for occlusion area. He focused on un-occluded and less occluded part of the face for feature extraction using the perceptron neural network whereas full face features were obtained through residual network. Both the features were weighted and fused and verified over two datasets. Wei-Jong Yang et al. [13] extended the capability of linear regression classification (LRC) by dividing the face into small sub faces (modules). They used the occluded part and as many as non-occluded part and analysed the texture histograms of the modules and then measured the HT difference. Thus the occlusion problem was solved using the weighted module LRC over two datasets. An occluded expression recognition model based on the generated countermeasure network was proposed in [14].

Some regions are invisible or the boundaries are blurred due to occlusion problem which give rise to insufficient information over the face region and consequently causes missed detection and low recalls. Many such works concentrated on context information and have obtained good results in the occlusion problem, therefore using context information is feasible. The work proposed in [15-16] suggests recovering the occluded part to increase the capability of face recognition system whereas [17] concentrated on excluding the occluded part from the face. The de-occlusion terminology poses significant challenge to secure the true identity of an individual, which may further degrade the face recognition rate. Thus test faces under occlusion have attracted attention of researchers from the Biometric Research Committee especially during the COVID-19 pandemic. Some of the sample images from the CelebA dataset are shown in figure 1.

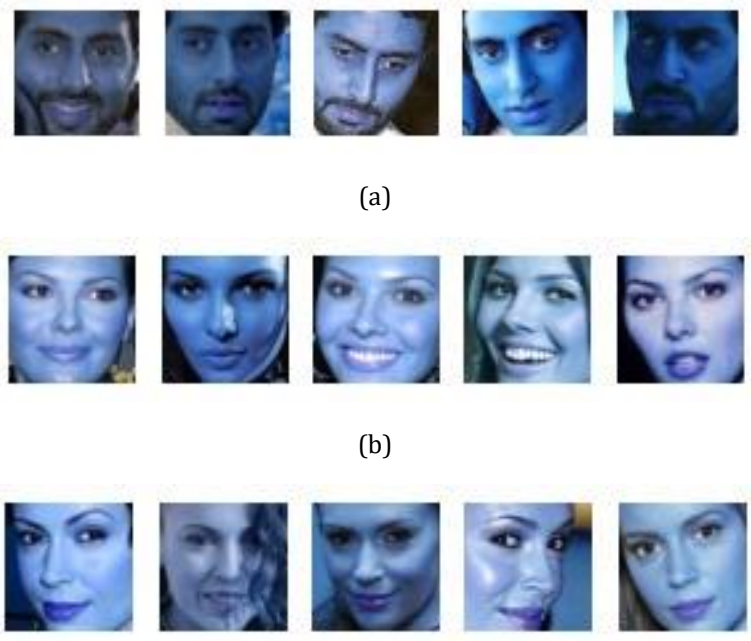

Fig. 1: Sample of images from CelebA Dataset. Different poses of (a) Abhishek Bacchan, (b) Ali Landry and (c) Alyssa Milano

The contributions of this paper are listed as follows:

1. The performance of SVM classifier was improved using robust optimum feature set. Local and Global features including textures were extracted from the occluded face region. For optimum quality features, the face region was contrast measured using Tadmor and Tolhurst technique and then contrast corrected for proper illumination. In addition the images were filtered to enhance and uplift the edges.
2. The robust feature set comprise of global features, patch based features, depth features, first order statistical features to decimate the effect of occlusions.
3. Optimum features extracted are based on Gabor coefficients, Linear Binary Patterns based on Haar Wavelet components, Histogram of Gaussian features. Statistical global features based on first order, wavelet components and color histograms were added to overcome the occluded region obstacles.

Related Work

Occluded face detection schemes aims basically in detecting the facial region covered by other objects. Most common approach involves partitioning the face regions into disjoint patches and then analysing them whether the patches belong to non-occluded or occluded part of the face region. Occlusion due to sunglasses and scarf was dealt in [18] by Min et al. where they divided the face region in two equal parts. They used Gabor features and PCA with SVM to classify the images. The work carried in [19] used a PCA model to determine whether a patch belongs to the occluded part after portioning the face region into non-overlapping patches. Occlusion in local regions was analysed using a probabilistic method by Martinez [20]. An ensemble classifier with probabilistic voting was introduced in [21]. The face region was calibrated using face alignment and a discrete wavelet filter was used to process the upper frequency coefficients to obtain a discriminative residual image. The color residue was further converted to YCbCr model and texture information was extracted using a texture descriptor. They used four CASIA datasets (FASD, MSU, ROSE-YOUTU and ROSE) and applied their work on intra and inter dataset test samples. Work in [22] suggested Fuzzy-SVM classifier to classify self-generated dataset acquired in different directions and angles. The images were pre-processed to extract the region of interest and HOG features were extracted. LPQ features were simultaneously obtained to use its blur invariant property over rectangular regions. They showed that their model have low time complexity and possess the ability to efficiently recognize different genuine and spoofed attacks due to HOG-LPQ property under blurring objects.

The authors in [23] used the chromatic texture difference between the real and forged images and extracted inter channel chromatic co-occurrence LBP (CCoLBP) and intra channel facial textures for presentation attacks. A softmax classifier with the inter and intra channel based features was used to evaluate the performance against testing samples from cross datasets (MSU MFSD, CASIA FASD, Replay Attack, Replay Mobile and OULU-NPU). They showed that their model improves the detection generalize ability using mutual information and discriminating power analysis. Later they combined CCoLBP with ensemble learning to analyse the chromatic discrepancies and reduce the effect of inter class imbalance between real and forged images [24].Zinelabidine B. et al. [25] extended the use of SURF features from grayscale to color images by applying it on each of the color bands separately. They concatenated the rotation invariant SURF features and then reduced them using PCA and Fisher vector encoding in order to reduce the computational complexity. The descriptor were obtained using a haar wavelet on a 4x4 blocks or sub-regions around a point of interest on RGB, HSV and YCbCr color spaces which were further concatenated to form a CSURF feature vector of dimension 64. They concluded that their approach even with limited training set on inter-dataset samples showed interesting generalization performance.

Methods and Material

We have used the traditional method for classifying the occluded faces (pose variation) from the CelebA dataset using course and fine features using various descriptors. The course features included features obtained using first order statistical features, color histogram based features and wavelet based magnitude and energy components whereas fine features include texture features obtained using Gabor, Haar mother wavelet Linear Binary Pattern, and Histogram of Gaussian based features. The occlusion over the face region imposes a great challenge for any classifier network. Therefore, the only remedy was to uplift quality distinguishable features from the faces. We have tried variety of pre-processing and features based on them without destroying the textural and structural aspect of the faces and experimentally optimized the pre-processing and the feature set to obtain best accuracy with such low frequency dataset corresponding to each class. Few faces and high number of classes was another constraint imposed for this new occluded face detection dataset. SVM was able to classify each class accurately due to diverse feature set which included both the statistical and textural features. Figure 2below shows the block diagram of the proposed occluded face identification system.

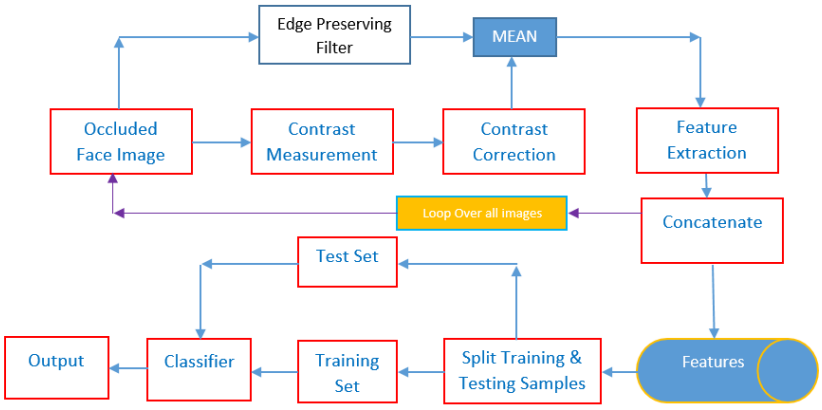

Fig. 2: Block diagram of the proposed occluded face identification system

Contrast Measurement & Contrast Correction

The CelebA face dataset was used with its original set of images for each subject. The techniques override data augmentation and able to distinguish the test image accurately. The contrast of the image as perceived by human is influenced by the spatial arrangements and the viewing conditions. Therefore, the measurement of the contrast becomes a complex approach. Basically, factors like illumination, resolution, color contents, eye distance etc. affects the contrast of the image when perceived. Contrast is the measure obtained through the difference between brightest and the darkest point [26]. Many such contrast measuring approaches are listed in the literature which involves both the local and the global techniques. One such global approach is suggested by Tadmor and Tolhurst [27] for measuring the contrast in images. The concept of difference of Gaussian (DOG) filtering is extended by Tadmor and Tolhurst where the following expression (1) for contrast measurement CM is suggested. Figure 3 shows the output obtained using contrast correction approach.

$$CM\,(x,y) = \frac{R_c(x,y) - R_s(x,y)}{R_c(x,y) + R_s(x,y)} \quad (1)$$

Where, the output of central component is,

$$R_c(x,y) = \sum_{i=x-3r_c}^{i=x+3r_c} * \sum_{j=y-3r_c}^{j=y+3r_c} Center\,(i-x, j-y) I(i,j) \quad (2)$$

While the output of surround component is,

$$R_s(x,y) = \sum_{i=x-3r_c}^{i=x+3r_c} * \sum_{j=y-3r_c}^{j=y+3r_c} Surround\,(i-x, j-y) I(i,j) \quad (3)$$

And the center and surround components of the receptive field is given by,

$$Center\ (x,y) = exp\left[-\left(\frac{x}{r_c}\right)\left(\frac{x}{r_c}\right) - \left(\frac{y}{r_c}\right)\left(\frac{y}{r_c}\right)\right] \quad (4)$$

(x,y) is the spatial coordinates of the receptive field, r_c is the radius at which the sensitivity decreases to *1/e* w. r. t. the peak level.

$$Surround\ (x,y) = 0.85\left(\frac{r_c}{r_s}\right)exp\left[-\left(\frac{x}{r_s}\right)\left(\frac{x}{r_s}\right) - \left(\frac{y}{s}\right)\left(\frac{y}{r_s}\right)\right] \quad (5)$$

Such that $r_s > r_c$.

Fig. 3: Contrast measurement using Tadmor and Tolhurst method and correction

The objective of measuring the image contrast is to correct the contrast. The issue is important when image features are extracted for classification problem. The classification accuracy is function of quality features which are governed by image contrast. Most of the benchmark datasets are prone to poor contrast images and need to be enhanced with respect to their contrast. A simple technique for contrast correction is utilized to obtain better classification for occluded faces where the Celebrity dataset contains obstacles over the face in various manners. We found that the following approach is able to uplift prominent features from the images after they were corrected in terms of contrast. The correction is applied to all the three color channels of an image and later combined. The following equations from (6) to (8) are used to correct the contrast of images where CM was evaluated using equation 1.

$$M = 255*CM \quad (6)$$

$$Factor = 259 * \frac{(M+255)}{(255*(259-M))} \quad (7)$$

$$G = (Factor * (I - 128)) + 128 \quad (8)$$

Edge Preserving Enhancement

Basically, anisotropic diffusion was introduced for denoising while preserving edges. Images are not only noisy but distorted to less or greater extent depending upon various natural factors and chemical compositions of colours. Therefore, the focus of diffusion scheme is not only to clear the noise but also to strengthen the edges. Work introduced by [28] [29] extended anisotropic diffusion to patch level. Authors in [29] introduced an edge preserving and denoising filter for 2D and 3D images and extended it to patches for feature extraction. The framework considers a color image in a hybrid special-spectral 5D space {x, y, R, G, B}. The filter requires two tuning parameters and includes the time step for stability (Usually set to the reciprocal of the squared number of dimension) and iterations for which the filter operates. Beltrami filter is capable of removing aliasing and weak textures while preserving the edges fine structure. We used the filter on high frequency enhanced grayscale image A' obtained with 15 iterations and time step of 0.25 to obtain the filtered image 'E'.

$$E = Bf(A', iterations, time\ step) \quad (9)$$

Where, Bf is the Beltrami filter function, A' is the high frequency enhanced image, iterations = 15 and time step = 0.25.

Both the figures of Abhishek Bacchan indicated in figure 4 do not show any remarkable change as considered with visual perception but the value of peak signal to noise ratio indicate the change.

Fig. 4: Edge Preserving filter output. PSNR = 41.3340

The final image used for feature extraction is obtained by averaging the output after contrast correction and the edge enhancing Beltrami filter.

Feature Extraction

We used Gabor features developed by [30] with default parameters including number of scales and orientations equals to 5 and 8, number of rows and columns of gabor filter to be 39. The rows and columns were down-sampled by a factor of 39. The image was converted to grayscale and 640 features were extracted.

Five first order statistical features were extracted from the grayscale image which includes mean, variance, standard deviation, skewness and kurtosis. These features are function of probabilities of pixel intensities in the facial region. The following are the expressions for each of the statistical feature components. The probability *P* corresponding to each of the intensity level is evaluated by the following expression (11) first and then mean, variance, standard deviation, skewness and kurtosis are evaluated using expressions (12) to (16)

$$G_L = 0{:}255 \tag{10}$$

$$P_{(x = 1 \text{ to } 255)} = \frac{1}{M*N}\sum_{i=1,j=1}^{i=M,j=N}(I_{img}(i,j) == x) \tag{11}$$

$$Mean = \sum G_L .* P \tag{12}$$

$$Var = \sum([(G_L - Mean)^2].* P) \tag{13}$$

$$Stdev = \sqrt{Var} \tag{14}$$

$$Skewn = \frac{\sum([(G_L - Mean)^3].*P)}{(Stdev^3)} \tag{15}$$

$$Kurts = \frac{\sum([(G_L - Mean)^4].*P)}{(Stdev^4)} \tag{16}$$

Mother wavelets such as bior (*bior 3.1, bior 3.5 and bior 3.7*), debauchees 3 (*db3*), symlet 3 (*sym3*) and *haar* were usedto extract wavelet based features from the contrast corrected grayscale image decomposed to single level. Two components especially the vertical and the diagonal were considered for magnitude and energy of the wavelet components. The following expressions (17) and (18) respectively find the magnitude and the energy component of the two decomposed components for course features.

$$W_M = \frac{1}{p*q}\left(\sum_{r=1}^{p}\sum_{c=1}^{q} W_x\right) \tag{17}$$

$$W_E = \frac{1}{p*q}\left(\sum_{r=1}^{p}\sum_{c=1}^{q} abs({W_x}^2)\right) \tag{18}$$

Where, p and q are the row and column dimension of the wavelet components. W_x is either W_v or W_d and corresponds to vertical and diagonal components. The total features obtained using six mother wavelets were 24.

The color frames corresponding to *RGB* image and the *Lab* color space image are considered to find histograms using 16 binary levels. These histograms were normalized using the dimension of the image. The expressions (19) and (20) below are used to extract features in color domain. Further the features from *RGB* and *Lab* color space were concatenated.

For *RGB* image,

$$H_{(x \in R, G, B)} = \frac{1}{M*N}H\,(I_{img}\,(x)) \quad (bins = 16) \tag{19}$$

For $LabI_{img}$ image,

$$H_{(y \in L, a, b)} = \frac{1}{M*N}H\,(I_{img}\,(y)) \quad (bins = 16) \tag{20}$$

LBP features are the most efficient features when classification is concerned. It not only lift the textural properties of the image but also capture details such as edges, patterns, illuminations etc. We used LBP over the color

image on its components and the features were then averaged. We also decomposed the color image to 4 level wavelet transform and LBP features from all its wavelet components were similarly averaged. Finally, the features from the original color image and its wavelet tributaries are averaged in the end. This ensures that none of the detail is lost and thus will help to distinguish between the image classes. Figure 5 depicts the mechanism for feature extraction using LBP.

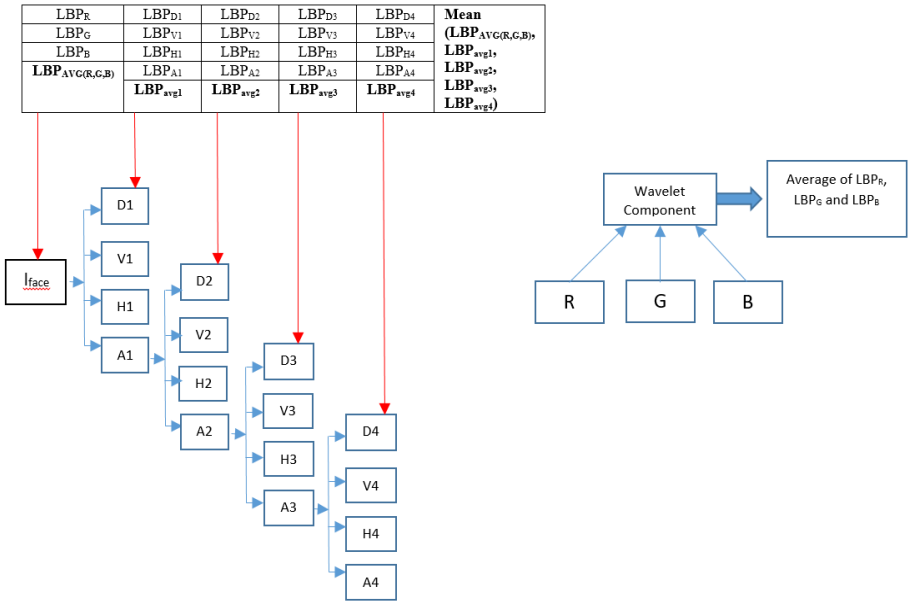

Fig. 5: LBP feature extraction mechanism using 'haar' wavelet. Each of the wavelet component has three color components viz. R, G and B.

We considered HOG features on image and on each color component of the image. We combined all four HOG features by averaging them and obtained them with cellsize set to [16 16].Table 1 and figure 6 lists the complete feature set and their dimensions consisting of coarse and fine features which were extracted in sequence as per the input given to the classifier SVM.

Table 1: Table showing the coarse and fine features extracted from images after contrast correction

Sr. No.	Name of the feature	Dimension
1	Gabor features	640
2	First order Statistical features	9
3	Wavelet based features – 6 Mother Wavelets	24
4	Color histogram based features	32
5	Haar wavelet based LBP features	59
6	Histogram of Gaussian based features	1764
	Total features	**2528**

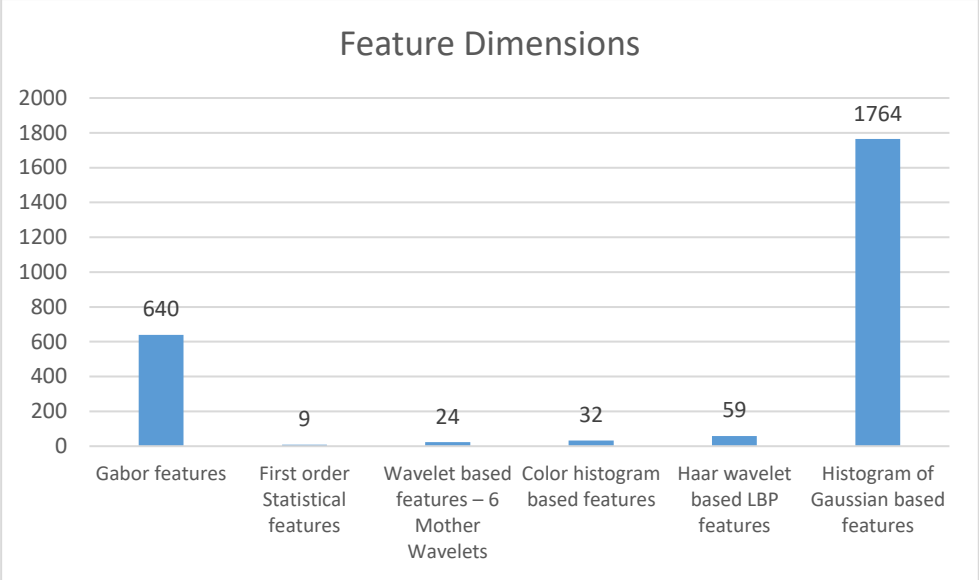

Fig. 6: Feature Set obtained from Occluded faces of the Dataset and their respective dimensions

Experimental Results

The CelebA Attributes Dataset (CelebA) [31] consists of 150 folders respective to 150 celebrities from all over the globe. Each folder includes images of different number of count with large diversities including pose variations and background clutter. We have selected 100 folders for our work for classification and without augmentation in its original form. The lowest and highest count of images from 100 folders is 7 and 403 respectively for folder 11 and 91. We restricted the maximum count to 240 which were conditioned on folder 20 and 91. The total number of images from all 100 folders was 11639. All the images were contrast corrected and edge enhanced and then the mean images were subjected to feature extraction process. Total 2528 features corresponding to each of the 11639 images were extracted and normalized.

SVM classifier with '*rbf*' kernel was used for classification. We tested our approach under different test set selection criteria. Two criteria's corresponding to selection of classes/folders based on count of images in each class/folder and percentage of test samples to be selected from the former threshold. Classes having number of samples/images greater than C = [5, 10, 20, 50, 75, 100, 125, 150 and 200] and percentage test samples/images in TH = [50%, 40%, 30%, 25%, 20%, 15% and 10%] were selected. The number of classes selected, total test samples/images corresponding to each of the criteria and the classification accuracy is depicted in table 2. The minimum accuracy obtained was 87% when 50% of data was used respectively for training and testing in all possible cases. The minimum accuracy obtained for classes having samples greater than C = 50 was 98% for TH = 30% test samples while the accuracy reduced to 94% for C = [20 and 10] and 93% for C = 5 when percentage of test samples were TH = 30%. Table 2 shows the classification accuracy with respect to percentage of test samples for each criteria marked with red color for TH = 30% and blue color for TH = 10% respectively.

Table 2: Classification Accuracy corresponding to sample threshold for individual folder/class and percentage of test samples

Number of Images in Individual folder greater than	Percentage of sample images from each selected folder	Number of such folders in 100 folders	Total number of test sample images	% Classification Accuracy
5	0.50	100	3664	87
	0.40		2911	90
	0.30		2167	**93**
	0.25		1813	94
	0.20		1437	94
	0.15		1063	95
	0.10		691	**95**
10	0.50	99	3661	87
	0.40		2909	91
	0.30		2165	**94**
	0.25		1812	94
	0.20		1436	95
	0.15		1062	95
	0.10		691	**95**
20	0.50	95	3632	87
	0.40		2886	91
	0.30		2150	**94**
	0.25		1798	94
	0.20		1426	95
	0.15		1056	96
	0.10		687	**96**
50	0.50	67	3138	94
	0.40		2497	98
	0.30		1864	**98**
	0.25		1556	98
	0.20		1236	98
	0.15		918	99
	0.10		600	**99**
75	0.50	46	2485	96
	0.40		1980	98
	0.30		1478	**99**
	0.25		1233	99
	0.20		981	99
	0.15		730	99
	0.10		477	**100**
100	0.50	19	1315	99
	0.40		1047	99
	0.30		785	**99**
	0.25		653	99
	0.20		520	99
	0.15		389	100
	0.10		258	**100**
125	0.50	09	764	99

	0.40		609	99
	0.30		457	**99**
	0.25		380	100
	0.20		303	100
	0.15		226	100
	0.10		150	**100**
150	0.50	03	356	100
	0.40		284	100
	0.30		213	**100**
	0.25		178	100
	0.20		142	100
	0.15		106	100
	0.10		71	**100**
200	0.50	03	356	100
	0.40		284	100
	0.30		213	**100**
	0.25		178	100
	0.20		142	100
	0.15		106	100
	0.10		71	**100**

Analysis over table 2 shown in table 3 indicates that our approach was able to perform better when C=50 (classes having samples greater than 50) for TH = 30% test samples with an accuracy in the range 98% to 100%.

Table 3: Classification Accuracy corresponding to sample threshold for individual folder/class with 30% and 10% test samples

Number of Images in Individual folder greater than	% of Test samples	Min – Max % Accuracy
5	30/10	93/95
10		94/95
20		94/96
50		98/99
75		99/100
100		99/100
125		99/100
150		100/100
200		100/100

We have compared our performance with state of art methods with respect to classification accuracy. The difference between other approaches listed in table 4 is the number of classes considered for training and testing. We have used only 100 classes for training and subsequently testing from 150 classes. Most of the techniques used in current literature is concentrated in deep and machine learning approaches. The table shows that our technique performs better than all other approaches achieving 98% classification accuracy.

Table 4: Comparison of proposed classification approach with other state of art techniques

Authors	Year	Method	Accuracy
Ching-Hao Chiu et al. [32]	2023	multi-exit (ME) training framework and the early exit policy for Deep Neural Network	85.3
EsubeBekele et al. [33]	2019	Modified Resnet Architecture	66.67
LiangqiongQu et al. [34]	2022	Federated Learning with Vision Transformers (VIT-FL)	Approx. 93
Junhyun Nam et al. [35]	2022	Spread Spurious Attribute	93
Ingrid Hrga et al. [36]	2022	Data Augmentation Techniques Inspired by Neural Architectural Search with MobileNet v3	92.79
Ours Approach	2023	Diverse features based SVM approach	98

Conclusion

In spite of scarce samples/classes in the CelebA dataset and the challenges in respect of large diversities, our traditional approach of feature based classification using SVM proved better than other advance methods such as deep learning and machine learning approaches. Though, we have not augmented the dataset and used it in its original form, the low count classes have no significant effect on classification. Nearly 4% feature dimension (2528) of the total dimension of the image size (256 x 256 = 65536) was successful to train the classifier due to optimum selection of coarse and fine features. The preprocessing (contrast correction and edge enhancement) is another fruitful stage of this work. The idea of considering the average image after two parallel pre-processing stages helped in acquiring efficient features. The approach can be used over other occluded face datasets with or without augmentation using finely tuned sophisticated classifiers. We have not focused on eliminating the region outside the region of interest (face region) since the area concerned is very less proportionally to the face region. We have tried other traditional features and along the features used in this work but they were not found significant. More fine structure-texture feature extraction techniques would contribute better and would increase the classification rate.

References

[1] Sun Y, Liang D, Wang X, Tang X (2015) Deepid3: Face recognition with very deep neural networks. arXiv:1502.00873

[2] Nash S, Rhodes M, Olszewska JI (2016) Ifr: Interactively pose corrected face recognition. In: Proceedings of the 9th International Joint Conference on Biomedical Engineering Systems and Technologies - BIOSIGNALS, (BIOSTEC 2016). INSTICC, SciTePress, pp 106–112.

[3] Olszewska JI (2016) Automated face recognition: Challenges and solutions. Pattern Recognition-Analysis and Applications, 59–79

[4] Kumar A, Kumar M, Kaur A (2021) Face detection in still images under occlusion and non-uniform illumination. Multimedia Tools Applications, 80(10):14565–14590

[5] Wang J, Yuan Y, Yu G (2017) Face attention network: An effective face detector for the occluded faces. arXiv:1711.07246

[6] Martinez, A.M., Kak, A.C.: PCA versus LDA. IEEE Trans. Pattern Anal. Mach. Intell. 23(2), 228–233 (2001)

[7] Ahonen, T., Hadid, A., Pietikainen, M.: Face recognition with local binary patterns. In: European Conference on Computer Vision, pp. 469–481. Springer, Berlin (2004)

[8] Mika, S., Ratsch, G., Weston, J., Scholkopf, B., Mullers, K.R.: Fisher discriminant analysis with kernels. In: Neural Networks for Signal Processing

IX: Proceedings of the 1999 IEEE Signal Processing Society Workshop, pp. 41–48. IEEE, Piscataway (1999)

[9] Heisele, B., Ho, P., Poggio, T.: Face recognition with support vector machines: Global versus component-based approach. In: Proceedings of IEEE 8th International Conference on Computer Vision (ICCV), pp. 688–694. IEEE, Piscataway (2001)

[10] Naseem, I., Togneri, R., Bennamoun, M.: Linear regression for face recognition. IEEE Trans. Pattern Anal. Mach. Intell. 32(11), 2106–2112 (2010)

[11] G. Rajeshwari and P. Ithaya Rani, "Face occlusion removal for face recognition using the related face by structural similarity index measure and principal component analysis," Journal of intelligent and Fuzzy Systems: Applications in Engineering and Technology, vol. 42, issue 6, 2022, pp. 5335-5350.

[12] Yueying Li, " Face detection Algorithm Based on Double-Channel CNN with Occlusion Perceptron, " Computational Intelligence ans Neuroscience, volume 2022, Article ID 3705581.

[13] Wei-Jong Yang, Cheng-Yu Lo, Pau-Choo Chung and Jar Ferr Yang, "Weighted Module Linear Regression Classifications for Partially-Occluded face recognition," Digital Image Processing Applications, Apr. 2022, doi: 10.5772/intechopen.100621.

[14] HuilinGe, Zhiyu Zhu, Yuewei Dai, Biao Wang and Xuedong Wu, "Facial expression recognition based on deep learning," Computer Methods Program Biomed, March 2022, 215, 106621.

[15] VijayalakshmiA.. Recognizing Faces with Partial Occlusion using Inpainting. *International Journal of Computer Applications* 168(13):20-24, June 2017.

[16] Min Zou, Mengbo You and Takuya Akashi, "Reconstruction of Partially Occluded Facial Image for Classification," Transaction on Electrical and Electronics Engineering, volume 16, Issue 4, pp. 600-608, 2021.

[17] Ashraf A. Maghari, "Recognition of partially occluded faces using regularized ICA," Inverse Problem in Science and Engineering, volume 29, issue 8, pp. 1158-1177, 2020.

[18] H. JunOh, K. MuLee, and S. UkLee, "Occlusion invariant face recognition using selective local non-negative matrix factorization basis images," Image and Vision Computing, vol. 26, no. 11, pp. 1515–1523, 2008.

[19] R. Min, A. Hadid, and J.-L. Dugelay, "Improving the recognition of faces occluded by facial accessories," in Proc. FG, 2011, pp. 442–447.

[20] A. M. Mart´ınez, "Recognizing imprecisely localized, partially occluded, and expression variant faces from a single sample per class," IEEE Trans. Pattern Anal. Mach. Intell., vol. 24, no. 6, pp. 748–762, 2002.

[21] Du Yuting, Qian Tong, Xu Ming and ZhengNing. (2021). Towards face presentation attack detection based on residual color texture representation. Security and Communication Networks, Volume 2021.

[22] K. Mohan, P. Chnadrashekhar and K. V. Ramanaiah. (2020). Object-specific face authentication system for liveness detection using combined feature descriptors with fuzzy-based SVM classifier. International journal of computer aided engineering and technology, volume 12(3), pp. 287-300.

[23] Peng F., Qin L. and Long M. (2018). CCoLBP: Chromatic Co-Occurrence of Local Binary Pattern for Face Presentation Attack Detection. 27th International Conference on Computer Communication and Networks (ICCCN), pp. 1-9.

[24] Peng F., Qin L. and Long M. (2020). Face presentation attack detection based on chromatic co-occurrence of local binary pattern and ensemble learning. J. Vis. Commun. Image R., volume 66, 102746.

[25] BoulkenafetZinelabidine, KomulainenJukka and HadidAbdenour. (2017). Face Antispoofing using Speeded-Up Robust Features and Fisher

Vector Encoding. Signal Processing Letters, IEEE, volume 24(2), pp. 141-145.

[26] Simone Gabriele, Pedersen Marius and Hardeberg John Yngve. (2012). Measuring perceptual contrast in digital images. Journal of Vis. Communication R., volume 23, pp. 491-506.

[27] Tadmor Y. and Tolhurst D. (2000). Calculating the contrasts that retinal ganglion cells and LGN neurones encounter in natural scenes. Vision Research, volume 40(22), pp. 3145–3157.

[28] Roussos and Maragos P. (2010). Tensor-based image diffusions derived from generalizations of the total variation and beltramifunctionals. In IEEE International Conference on Image Processing (ICIP), pp. 4141-4144, September 2010.

[29] Wetzler and Kimmel R. (2012). Efficient beltrami flow in patch-space. In Scale Space and Variational Methods in Computer Vision, volume 6667 of Lecture Notes in Computer Science, pp. 134-143. Springer Berlin/Heidelberg.

[30] Haghighat M., Zonouz S. and Abdel-Mottaleb M. (2015). CloudID: Trustworthy cloud-based and cross-enterprise biometric identification. Expert Systems with Applications, volume 42(21), pp. 7905-7916.

[31] Liu, Z.; Luo, P.; Wang, X.; and Tang, X. 2018. Largescalecelebfaces attributes (celeba) dataset. Retrieved August, 15(2018): 11.

[32] Ching-Hao Chiu, Hao-Wei Chung, Yu-Jen Chen, Yiyu Shi and Tsung-Yi Ho, "Fair Multi-Exit Framework for Facial Attribute Classification," 2023, http://openreview.net/forum?id=nY5e2_e7WpY.

[33] E. Bekele and W. Lawson, "The Deeper, the Better: Analysis of Person Attributes Recognition," *2019 14th IEEE International Conference on Automatic Face & Gesture Recognition (FG 2019)*, Lille, France, 2019, pp. 1-8, doi: 10.1109/FG.2019.8756526.

[34] LiangqiongQu, Yuyin Zhou, Paul Pu Liang, Yingda Xia, Feifei Wang, EhsanAdeli, Li Fei-Fei and Daniel Rubin, " Rethinking Architecture Design for Tackling Data Heterogeneity in Federated Learning," Proc IEEE ComputSocConfComput Vis Pattern Recognit. 2022 June ; 2022: 10051–10061.

[35] Junhyun Nam, Jachyung Kim, Jaeho Lee and Jinwoo Shin, "Spread Spurious Attribute: Improving Worst-group accuracy with spurious attribute estimation," ICLR, 2022.

[36] Ingrid Hrga and Marina Ivasic-Kos," Effect of Data Augmentation on Face Classification Results," In Proceedings of the 11th International Conference on Pattern Recognition Applications and Methods (ICPRAM 2022), pages 660-667.